BONDED REPAIR OF CFRP PRIMARY STRUCTURE: TESTING AND ANALYSIS OF BONDED SCARF JOINTS.

B. Twist[1*], J.C. Arnold[1], R.W. Jones[2], N.A. Khan[3]

[1]*Swansea University, College of Engineering, Swansea, Wales UK, SA2 8PP*
[2]*Airbus (A350-1000 demonstrators), Filton, Bristol, UK, BS99 7AR*
[3] *Imperial College London, Faculty of Engineering, South Kensington Campus, London SW7 2AZ*

bentwist@googlemail.com

Keywords: Repair, Adhesion, Composites, Scarf Joints.

Abstract
This paper presents test and analysis of secondary bonded scarf joints in carbon fibre / epoxy composites. The scarf joints were manufactured from composite material typical of that used in the latest generation of civil aircraft. Four 120°C cure epoxy film adhesives and 5 different scarf angles were tested. Photo-elastic analysis concluded that significant stress peaks were found at the bond line adjacent to the 0° ply interface and results were compared to failure predictions. Fractography and microscopy were used to characterise the failure mechanisms.

1 Introduction

1.1 Literature

The civil aircraft industry has invested heavily to replace existing aluminium primary structure with lighter, stronger and stiffer carbon fibre composites for the primary material used in the latest generation of civil aircraft [1]. To capitalise on the performance advantage of CFRP, far fewer rivets and bolts exist in the latest generation of aircraft. In order to perform a bolted repair multiple holes need to be drilled into the structure which causes significant damage with a load path that is far from ideal. The added weight of a repair plate can be significant and it can be difficult to find an aerodynamically efficient solution. Composites appear to be well suited to bonding even for primary components such as stringers, which are being bonded to the wing skin to give a stiff load path. Although bonded repairs offer similar advantages, they are not currently certified for structural repairs in large civil aircraft, however this is a topic of significant interest in recent years with civil aircraft requiring an alternative to bolted repair.

Previous research on the behaviour of bonded scarf joints has identified a knockdown in strength of 60% for a 1° scarf angle and a 89% knockdown for a 5° scarf angle. This was based a UD layup which gave two failure modes; a cohesive one and an interlaminar failure including fibre pull-out, or a combination of the two depending on the angle tested were seen in the UD layup [2]. Investigations on the stress distribution along the bond line of a bonded layup involving 0° and 90° plies showed a combination of peel and shear stresses [3], [4]. The main aim of this study is to provide more information on the effect of scarf angle on bond strength with a quasi isotropic layup with 4 epoxy film adhesives.

2 Experimental techniques

2.1 Test Material

The scarf joints were made from HEXPLY M21/T800 [5]. This material was chosen for the coupon material as it is representative of the high strength and stiffness 180°C cure materials used in primary structure for the latest generation of large civil aircraft. The film adhesives chosen to bond the scarf joints together were Hysol EA9695 [6], FM300-2M [7], FM300-2K [7] & Redux 312 [8]. These adhesives were chosen as they are high strength 120°C cure epoxy adhesives that are representative of the sort of material that could be used for primary structural repair on the next generation of civil aircraft.

2.2 Specimen Geometry

The specimen layup used was quasi isotropic consisting of 16 plies at 0.25mm per ply to give a nominal thickness of 4mm, as shown in figure 1 where L is the length of the coupon dependant on scarf angle α. Samples were manufactured using autoclave processing followed by NDT to ensure quality.

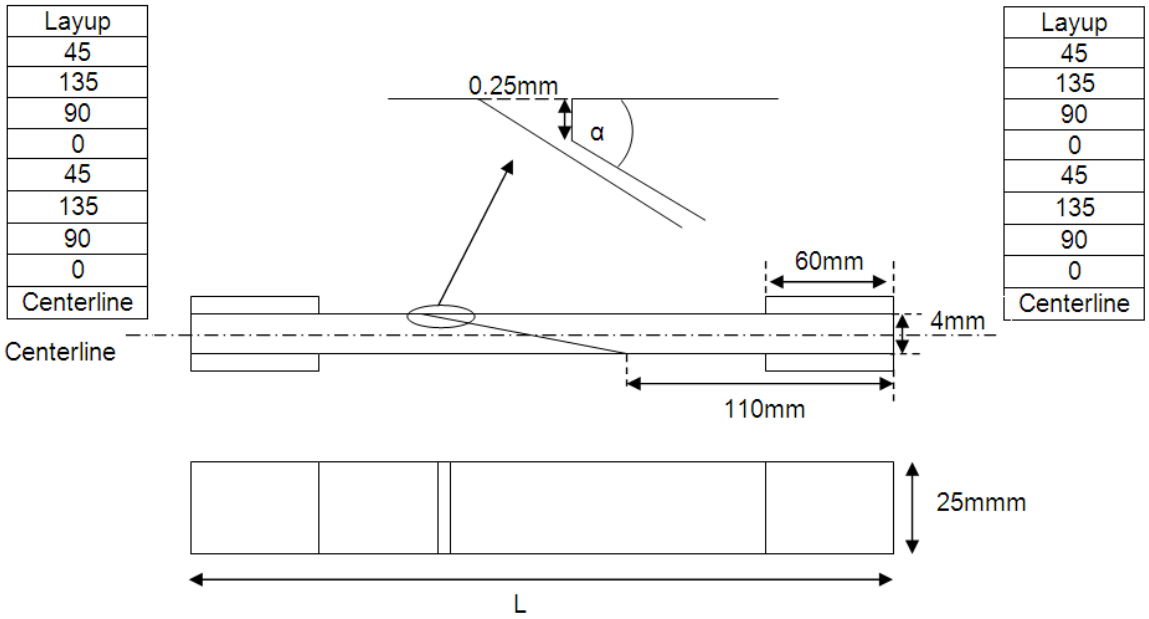

Figure 1. Specimen geometry and stacking sequence

2.3 Specimen Manufacture

Bonded specimens were produced, by first machining the samples using a 12mm diameter end mill inclined to the scarf angle leaving a single ply edge as shown in Figure 1. During machining, parts were held using a vacuum to prevent the part from warping. The sample width for the 4.5° and 7° specimens was 45mm wide compared to 25mm for the other scarf angles. It is assumed that the difference in the width of the coupons did not affect the results. The two machined parts underwent surface abrasion, surface cleaning with environmentally friendly cleaning wipes (with the exception of the Redux 312, for which acetone was used) and drying prior to bonding. The bonding of the two parts using the film adhesive was performed in an oven with cure conditions shown in Table 1 in line with manufacturer's recommendation under a vacuum of > 0.75 bar. End-tab material was 3mm thick Tufnol

sheets bonded with Araldite AB420 to the manufacturer's specification. Tensile testing was conducted in room temperature conditions using a 100kN Instron test machine. The tests were performed using displacement control with a cross head speed of 2mm /min.

Adhesive	Ramp rate (^{o}C per min)	Cure Temp (^{o}C)	Time at this cure temp minutes	Ramp down at ramp rate under vac until (^{o}C) then film adhesive can be released
EA 9695 [6]	3	120	120	40
FM300-2M [7]	3	120	60	40
FM300-2K [7]	3	120	60	40
Redux 312 [8]	3	120	30	40

Table 1. Cure information taken from material specifications

3 Predictive methods.

Predictive methods were derived using the lap shear strength of the adhesive. These methods assume cohesive shear failure within the adhesive and do not take into account any interlaminar or intralaminar failure that can occur at shallow scarf angles. For the purposes of this paper, only predictions using published data for EA9695 are shown. The lap shear strength of the material was quoted as 34.5MPa, against graphite substrates, cured at 177^{0}C. As this adhesive is a dual-cure material, its room temperature shear strength when cured at 120^{o}C is expected to be similar.

3.1 Average shear strength

The average shear strength prediction shown in equation 1 where P = Load, τ = average shear stress, t_{trim}= thickness of a trimmed laminate and d = depth of the specimen, as indicated in Figure 2. The assumption is that the average shear strength of the adhesive is applied over the length of the scarf region. A limitation of this method is that it does not take into account stress peaks and is therefore expected to be optimistic when used to predict failure loads.

$$P = \frac{\tau t_{Trim} d}{\sin\theta \cos\theta} \qquad \text{- (Equation 1)}$$

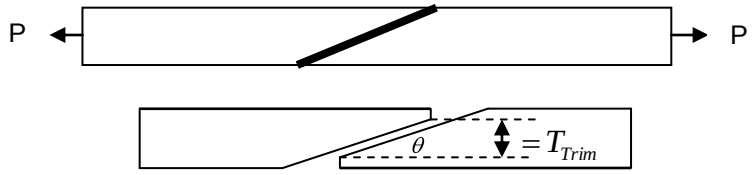

Figure 2. Force diagram & geometry diagram for scarf joint

3.2 Peak shear stress

The Peak shear stress prediction shown in equation 2 assumes that there are stress peaks in the region where the 0^o plies meet the bond line. Failure is assumed to occur when the shear stress in this area reaches the peak shear stress of the adhesive. This method is expected to be conservative as it does not allow for redistribution of load through the bond line once the

adhesive has gone beyond its elastic limit and assumes only a small proportion of the bond line is working.

$$P = \frac{\tau E_{Lam} t d}{E_0 \sin\theta \cos\theta}$$

- (Equation 2)

Where E_{Lam} = Modulus of the laminate, t = Thickness of the laminate and E_0 = Modulus of the 0_o plies. Results of both prediction methods are shown in Figure 4.

4 Test results.

The test matrix is shown in table 2 and results are shown in Figure 3. Figure 4 then shows individual test results for the 3° samples, showing the degree of sample variability.

Test Number	Loading	Scarf Angle (α) °	Film Adhesive	No. of Specimens RT/AR	Total Number of Tests
2 - 1	Tension	0.7	EA9695 0.5 NW	5	5
2 - 2	Tension	0.7	FM300 - 2K	5	5
2 - 3	Tension	0.7	FM300 - 2M	5	5
2 - 4	Tension	0.7	Redux 312	5	5
2 - 5	Tension	1.5	EA9695 0.5 NW	5	5
2 - 6	Tension	1.5	FM300 - 2K	5	5
2 - 7	Tension	1.5	FM300 - 2M	5	5
2 - 8	Tension	1.5	Redux 312	5	5
2 - 9	Tension	3	EA9695 0.5 NW	5	5
2 - 10	Tension	3	FM300 - 2K	5	5
2 - 11	Tension	3	FM300 - 2M	5	5
2 - 12	Tension	3	Redux 312	5	5
2 - 13	Tension	4.5	EA9695 0.5 NW	5	5
2 - 14	Tension	7	EA9695 0.5 NW	5	5
			Total Number of Tests	**70**	**70**

Table 2. Test matrix

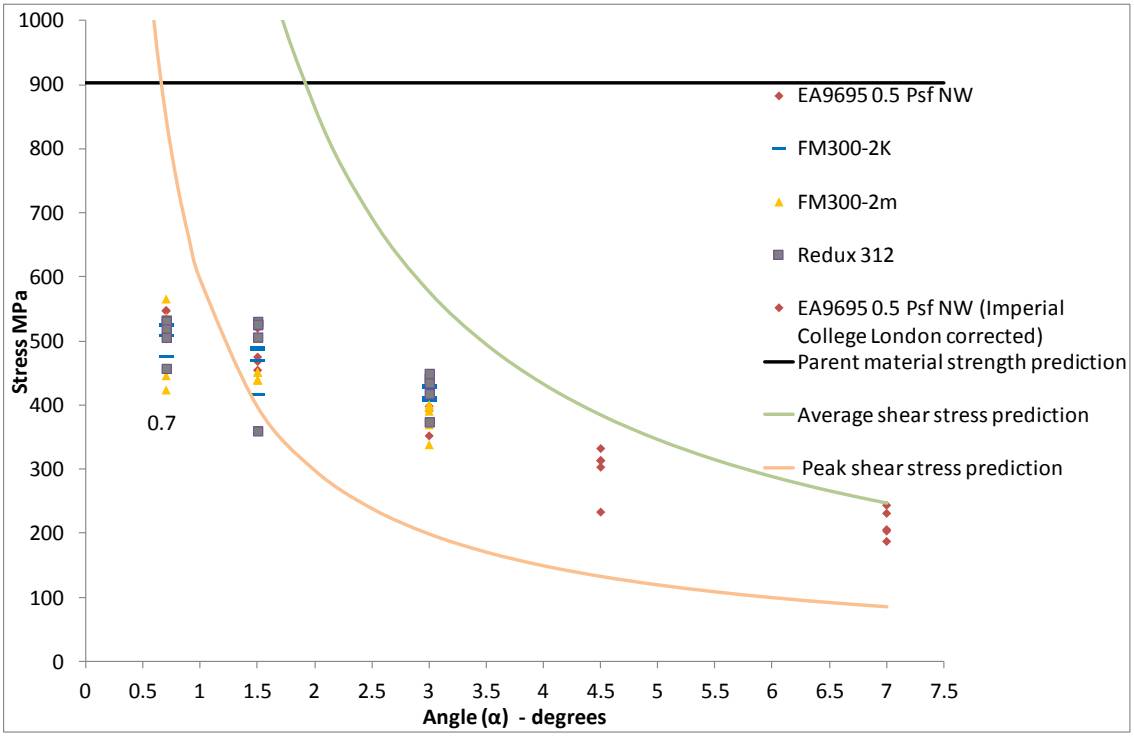

Figure 3. Scarf test results

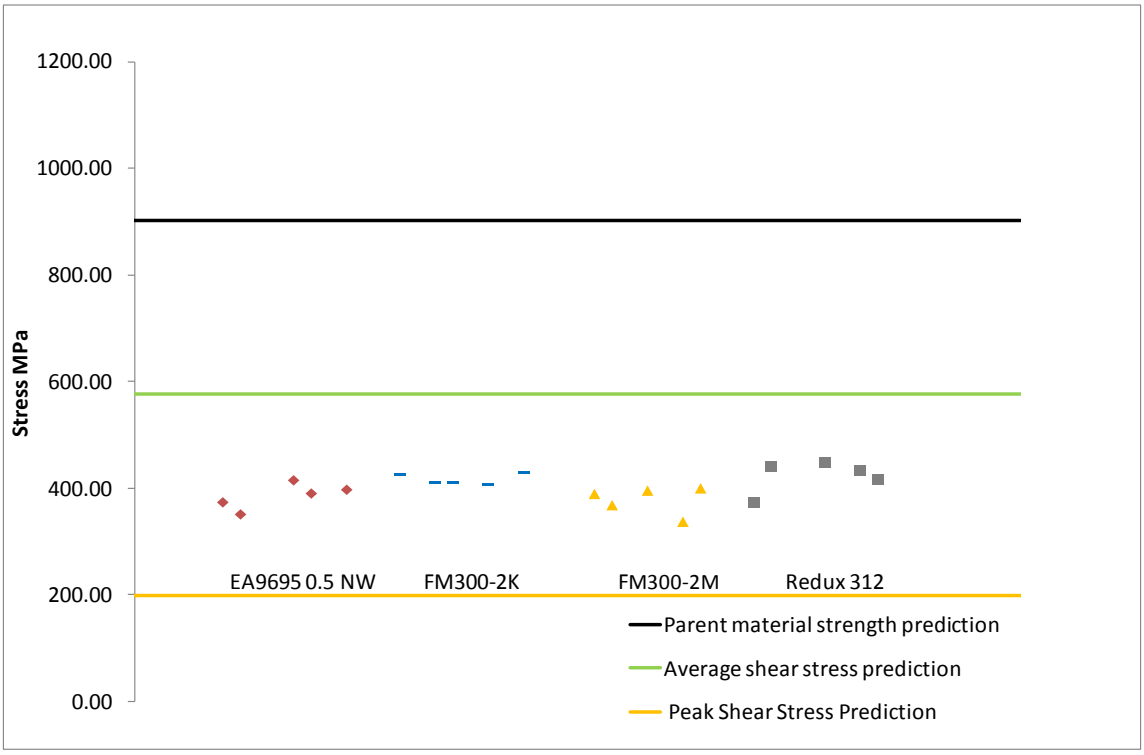

Figure 4. Individual test results for the 3° scarf angle samples.

5 Analysis

Fractography shown in figures 5-7 identified the failure modes and the likely initiation locations for the failure. Figure 8 shows cross sections through the bond with two adhesives showing differences at the feather edge. The failure modes varied with the scarf angle rather than the epoxy adhesive used. It is clear from the test results that the coupons that have scarf angles of 3^o and above exhibit a predominantly cohesive failure mode within the adhesive, apart from the 90^0 plies where matrix and fibres are pulled away, suggesting that the adhesives are stronger than the matrix epoxy of the composite. Although there is some scatter in the results, the shape of the two prediction methods used reflects the pattern of failures at these angles above 3^o with the failure load increasing as the scarf angle decreases. The peak shear stress prediction could be improved by using lap shear data from a shorter overlap or calculating the peak shear stress value on a shear stress curve which would then shift this line up towards the test results. The average shear stress method appears to be optimistic as expected, which is probably due to the failure being linked to the stress peaks at the 0^o ply bond line interface. The photo elastic analysis shown in figure 9 confirms the existence of these stress peaks and confirms that there are stress peaks at the feather edge of the repair. A reduction in these stress peaks would likely to improve the performance of the scarf joint. These peaks are similar to those shown in [4] and offer an explanation into likely failure locations.

Figure 5. Mode A = Cohesive failure except on the 90^o plies where fibre pull out is evident scarf angle 3^o adhesive Redux 312

Figure 6. Mode B = Fibre pull out, (interlaminar and intralaminar failure) scarf angle 0.7^o adhesive Redux 312

Figure 7. Net section failure (but at approx 50-60% of plain coupon failure load) scarf angle 0.7^o adhesive EA9695 0.5 psf.

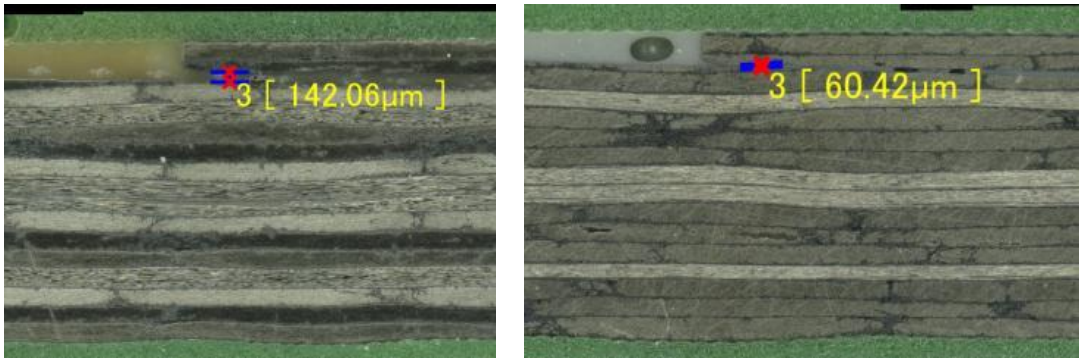

Figure 8. (Left) shows the feather edge of the a scarf joint with the FM300 –2K which has a knitted scrim. (Right) shows the Redux 312 which does not contain a scrim thus the bond line is very thin at the feather edge of the coupon.

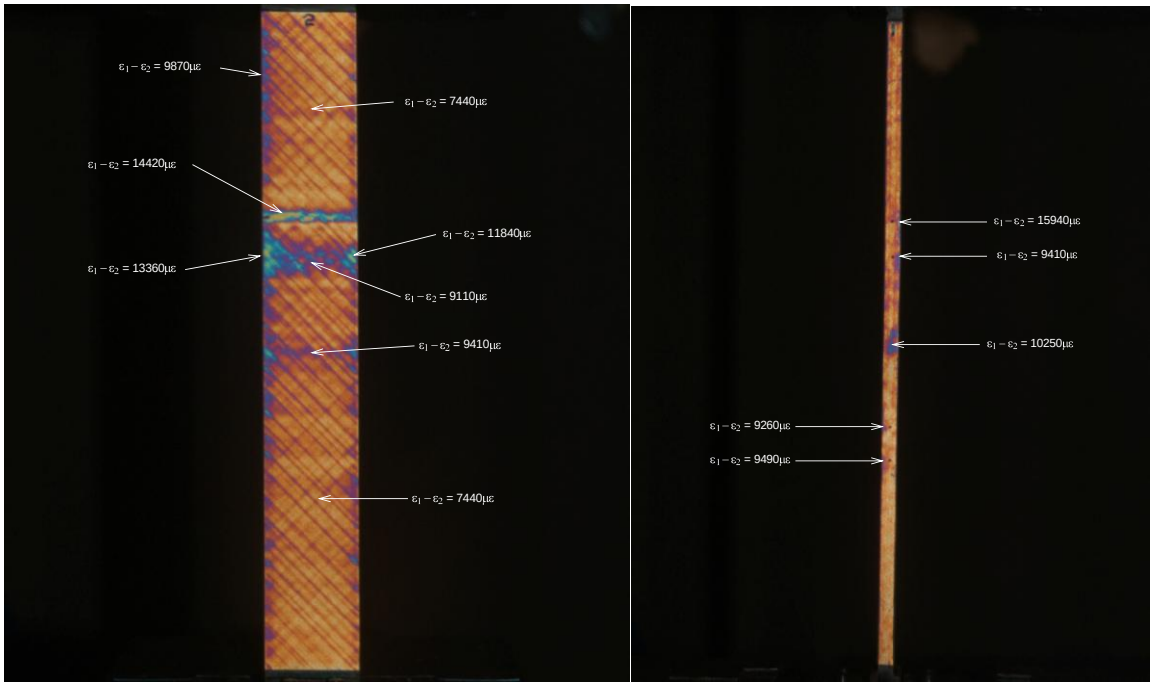

Figure 9 . Shows the stress peaks around the 0^o ply / bond line interface and the stress peaks at the scarf feather edge on a 3^0 coupon bonded with EA9695

Failure for the 1.5^o and 0.7^o scarf coupons is more complex and although failure initiates in the bond line, it doesn't follow the cohesive failure mechanisms of the of the scarf angles 3^o, 4.5^o & 7^o. For the 1.5^o scarf angles and a small proportion of the 0.7^o angles the failure mode appears to move from the bond line into an interlaminar / intralaminar failure within the composite matrix, with the initiation point being the 0^o fibre bond line interface. These failure modes are shown in [1] but appear to be layup dependent as they are seen at shallower angles than those observed in this paper. For the 0.7^o scarf angle coupons, the main failure mode was what appeared to be net section failure initiating in the 0^o ply / bond line interface midway through the length of the bond line. This would indicate that for this layup there are 3 failure modes of which 0.7^o is on the border between net section and fibre pull out. The shallower the angle, the less likely failure is to occur at the feather edge of the coupon. This is probably due to peel forces being reduced as the scarf angle reduces. There are some strength benefits from the use of shallow scarf angles below 3^o however the benefits of this has to be weighed up with the large amount of material removal required the extra size of the joint and the added

machining complexity. There seemed to be no major difference in failure mode or load with different adhesives.

The strength knockdowns seen in table 3 are significantly less than those seen in [1] this is highly likely to be due to the quasi isotropic layup of this test programme. In some samples, there was a higher than expected number of bond line voids. These did not appear to affect the tensile strength performance of the joint, with good tensile performance seen throughout. The knitted scrim used in the FM300-2K did seem to maintain the thickness of the adhesive much better than a limited scrim of the FM3000-2M. The voids did seem to be linked to the use of environmentally friendly surface wipes used during the preparation of the test specimens, hence the Redux 312 which used acetone had minimal void content.

Scarf Angle °	0.7	1.5	3	4.5	7
Strength knock down %	43	46	57	67	76

Table 3. Strength knock down based on the average test results for EA9695 film adhesive compared to the predicted plane tension coupon results.

6 Conclusion

In conclusion the failure mode and load of the scarf joints tested was entirely dependent on scarf angle. When approaching shallow angles, the failure mechanisms change so that they don't achieve the shear based stress predictions shown. The particular epoxy film adhesive used and whether or not porosity was found in the bond line in this case did not appear to influence the failure mode and load.

7 Acknowledgements

The authors would like to thank Airbus for providing the materials, manufacture of the coupons and photo elastic analysis, Swansea University for providing the use of the test machine and microscopy facilities and Imperial College London for the testing of the 4° and 7° scarf coupons.

References

[1] Edwards, T., Composite materials revolutionise aerospace engineering, in Ingenia. 2008: Online. p. 25-28.
[2] Kumar, S.B., et al., Tensile failure of adhesively bonded CFRP composite scarf joints. Materials Science and Engineering: B, 2006. 132(1-2): p. 113-120.
[3] He, D., et al., Stress analysis and strength evaluation of scarf adhesive joints subjected to static tensile loadings. International Journal of Adhesion and Adhesives, 2010. 30(6): p. 387-392.
[4] Campilho, R.D.S.G., et al., Modelling the tensile fracture behaviour of CFRP scarf repairs. Composites Part B: Engineering, 2009. 40(2): p. 149-157.
[5] HexPly® M21 data sheet, http://www.hexcel.com
[6] Hysol® EA 9695 data sheet, www.aerospace.henkel.com
[7] FM® 300-2 film adhesive technical data sheet, www.cytec.com
[8] Redux® 312 product data, http://www.hexcel.com